PHYSICAL REVIEW B VOLUME 31, NUMBER 8 15 APRIL 1985

Pressure dependence of elastic constants of $(V_{1-x}Cr_x)_2O_3$ at 296 K

H. Yang and R. J. Sladek
Department of Physics, Purdue University, West Lafayette, Indiana 47907

H. R. Harrison
Materials Research Laboratory, Purdue University, West Lafayette, Indiana 47907

(Received 19 November 1984)

Transit times of 30-MHz ultrasonic waves in $(V_{1-x}Cr_x)_2O_3$ single crystals, with nominal (actual) x values of 0.015 (0.013) and 0.030 (0.028), were measured at 296 K using hydrostatic pressures up to 4 kbar for $x=0.03$ and 1.2 kbar for $x=0.015$. The results were used to deduce 1-bar values and pressure derivatives of the elastic constants. Two of the elastic constants, C_{11} and C_{12}, have unusual negative pressure dependences resulting in both the λ_4 elastic eigenvalue and the bulk modulus B decreasing strongly with increasing pressure. The behavior of λ_4 indicates that pressure tends to make the lattice unstable toward a deformation which increases the c/a ratio without changing the crystal symmetry. This is consistent with the structural change at the pressure-induced, paramagnetic insulator-to-metal transition. For $(V_{0.97}Cr_{0.03})_2O_3$, we deduce a negative elastic γ which disagrees with its positive thermal γ whereas these γ's agree with each other in V_2O_3. These results are due to the elastic γ having strong negative contributions from some acoustic modes in certain directions in $(V_{0.97}Cr_{0.03})_2O_3$ but not in V_2O_3.

I. INTRODUCTION

The mixed transition-metal compound $(V_{1-x}Cr_x)_2O_3$ has been a subject of numerous investigations[1] in the past decade. Much of the work has been concerned with the electrical, structural, magnetic, thermal, and optical properties to characterize the nature of several phase transitions encountered in this system. From the electrical-resistivity measurements as a function of temperature[2–5] and pressure[2–4] for various Cr concentrations in V_2O_3, the phase boundary of the higher-temperature metal-insulator transition has been established as part of a generalized temperature-composition-pressure phase diagram[2–6] involving at least three different phase transitions. At room temperature, this first-order metal-insulator transition was found to occur at a critical composition of $x\sim0.01$ with concomitant discontinuous changes in lattice parameters[3,7] and interatomic distances,[7] but no change in the $R\bar{3}c$ crystal symmetry. It was also found that application of hydrostatic pressure to $(V_{1-x}Cr_x)_2O_3$ crystals with $x>0.01$ transforms them from the insulating phase into a metallic phase at a pressure which depends on the Cr concentration.[2–4]

The pressure dependences of elastic constants at low pressures have provided valuable information about lattice instabilities and have been used to estimate the pressures at which structural phase transitions occur in many crystals.[8,9] The $(V_{1-x}Cr_x)_2O_3$ system provides an excellent opportunity to investigate elastic behavior associated with a pressure-induced, insulator-to-metal (IM) transition which is not accompanied by a change in crystal symmetry. It should be noted that the study of elastic properties in this system has thus far been limited to pure V_2O_3,[10–14] due to the difficulties in growing $(V_{1-x}Cr_x)_2O_3$ single crystals with relatively large dimensions and good quality (i.e., without voids, cracks, etc.) which are required for ultrasonic investigations. The crystal-growth problem has been overcome by using a crucibleless, skull-melting technique[15] with a controlled CO_2-CO atmosphere to produce stoichiometric single crystals as large as $20\times10\times10$ mm^3.

When appropriate single-crystal samples suitable for ultrasonic velocity measurements became available, we began an investigation of the pressure dependence of the elastic constants for $(V_{1-x}Cr_x)_2O_3$ with nominal x values of 0.015 and 0.03. If the Cr substitution does indeed scale linearly with the effective negative pressure as suggested from empirical findings (i.e., 1 at.% Cr~-3.6 kbar),[2] the critical pressures for the IM transition at room temperature would be about 1.8 and 7.2 kbar, respectively, for $x=0.015$ and 0.03. To avoid possible damage to our $x=0.015$ samples at the IM transition, we employed pressures no larger than about 1 or 1.2 kbar and measured the pressure dependences of only C_{11}, C_{33}, and C_{44} moduli. These precautions were taken because for the $x=0.015$ sample with [100] faces the ultrasonic signal disappeared near 1 kbar, and was not recovered when the pressure was released. Subsequent microscopic examination of the sample revealed visible cracks similar to those observed at the IM transition as a function of temperature.[16] However, we were able to determine the pressure dependences of all the elastic constants for the $x=0.03$ sample up to 4 kbar.

II. EXPERIMENTAL PROCEDURE

Single-crystal samples of $(V_{1-x}Cr_x)_2O_3$ with nominal x values of 0.015 and 0.03 were prepared from the boules grown in the Central Materials Preparation Facility of the Purdue Materials Research Laboratory. The actual Cr concentrations of the crystals were analyzed[17] by atomic absorption spectroscopy and were found to be slightly smaller than the corresponding nominal values, namely 0.013 as compared to 0.015 and 0.028 as compared to 0.030. In the present paper the nominal concentrations will be used to specify x. The samples were oriented to within $\frac{1}{2}°$ using Laue x-ray backreflection and polished so as to have pairs of flat faces perpendicular to the threefold c axis, twofold a axis, and a direction 45° from the c axis in the mirror plane. The opposite faces were parallel to within 0.01°. The densities of the samples were determined by a liquid-immersion method to be 4.95 and 4.98 g/cm^3, respectively, for $x=0.015$ and 0.03, in good agreement with the value of 4.96 g/cm^3 deduced from x-ray work.[18]

Transit times of various 30-MHz ultrasonic waves were measured at 296 K by means of the standard pulse-echo-overlap technique[19] as a function of hydrostatic pressure up to about 4 kbar for the $x=0.03$ sample and up to 1.2 kbar for the $x=0.015$ sample. Transit-time—versus—temperature data near room temperature were also measured and used to correct the small effect of a slight temperature drift which occurred during each pressure run. Further experimental details on the pressure apparatus and bonding of the quartz transducers can be found elsewhere.[20]

III. DATA ANALYSIS AND RESULTS

The equations relating the directly determined moduli, $\rho v_i^2 (i=1-7)$, to the six independent elastic constants, $C_{\mu\nu}$, are given in the literature.[13,21] It is noted, however, that we used an opposite sign in front of each C_{14} term in the equations for C_T and C_{QT} moduli because the direction of wave propagation for these moduli was identified in the present study, following the convention adopted by Wachtman *et al.*,[22] as $(0, -1/\sqrt{2}, 1/\sqrt{2})$, which is different from the $(0, 1/\sqrt{2}, 1/\sqrt{2})$ direction employed in Ref. 13. For convenience we also note that the angles between the basal plane and the plane of polarization is $-7°$ for the fast transverse mode and 83° for the slow transverse mode in the case of the $x=0.03$ sample.

To determine the elastic-stiffness moduli as a function of pressure from our echo-overlap frequency data, we used equations taken from Ref. 23. It should be mentioned that for this calculation previous investigators[23–25] employed an incorrect relation between the adiabatic and isothermal compressibilities. This is usually of little practical consequence since the correction is extremely small because the adiabatic and isothermal compliances ordinarily differ by less than 1%.[26] To check on the situation in our samples we note that the correct relation[27] is

$$\beta^T_{\perp(\parallel)} = \beta^S_{\perp(\parallel)} + \alpha_{\perp(\parallel)}\alpha_V T/C_P \;, \tag{1}$$

where $\beta^T_{\perp(\parallel)}$ and $\beta^S_{\perp(\parallel)}$ are the isothermal and adiabatic compressibilities, respectively, perpendicular (parallel) to the c axis; $\alpha_{\perp(\parallel)}$ is the thermal-expansion coefficient perpendicular (parallel) to the c axis, $\alpha_V = 2\alpha_\perp + \alpha_\parallel$, and C_P is the heat capacity per unit volume at constant pressure. For the $x=0.03$ crystal, for example, $\alpha_\perp = 10\times10^{-6}/K$, $\alpha_\parallel = 4\times10^{-6}/K$,[28] and $C_P = 108$ J/mol K,[29] together with $\beta^S_\perp$ and $\beta^S_\parallel$ of 2.027×10^{-13} and 1.017×10^{-13} cm^2/dyn (calculated from the adiabatic elastic constants using the relations given by Nye[30]), results in the values of $\beta^T_\perp$ and $\beta^T_\parallel$ about 1.0% and 0.8% larger than that of the respective adiabatic ones.

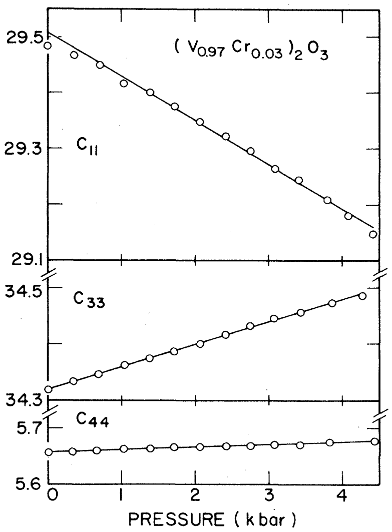

FIG. 1. Elastic-stiffness moduli C_{11}, C_{33}, and C_{44} of $(V_{0.97}Cr_{0.03})_2O_3$ as a function of hydrostatic pressure.

The adiabatic elastic-stiffness moduli determined for the $x=0.03$ sample are plotted in Figs. 1 and 2 as a function of hydrostatic pressure. All the pressure dependences are seen to be linear within experimental error. The solid lines represent the linear, least-squares fits to the data points. The values of six independent elastic constants $C_{\mu\nu}$ and their pressure derivatives $\partial C_{\mu\nu}/\partial P$, where $\mu\nu = 11$, 33, 44, 12, 13, and 14, were determined from $(\rho v_i^2)_{P=0}$ and $\partial(\rho v_i^2)/\partial P$, where $i=1-7$, by fitting, respectively, to the seven equations mentioned previously

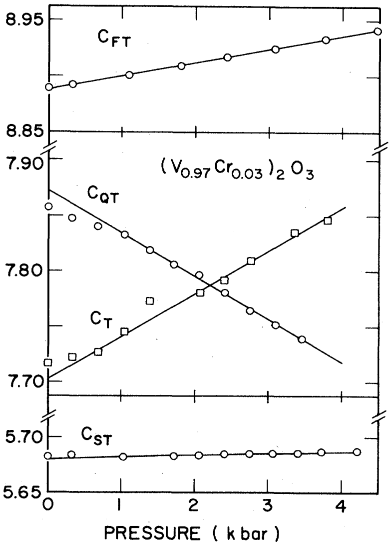

FIG. 2. Elastic-stiffness moduli C_{FT}, C_{QT}, C_T, and C_{ST} of $(V_{0.97}Cr_{0.03})_2O_3$ as a function of hydrostatic pressure. The subscripts stand for fast transverse, quasitransverse, transverse, and slow transverse, respectively.

TABLE I. Adiabatic elastic constants $C_{\mu\nu}$, bulk modulus B, and their pressure derivatives at room temperature of $(V_{1-x}Cr_x)_2O_3$ for $x=0$, 0.015, and 0.03. The values for $x=0$ (V_2O_3) are taken from Ref. 13.

	$x \diagdown \mu\nu$	11	33	44	12	13	14	B
C^a (10^{11} dyn/cm^2)	0	27.1	33.4	8.4	8.2	14.7	-1.9	17.2
	0.015	28.7	33.9	5.6	10.5	15.4	-0.3	18.8
	0.03	29.5	34.4	5.7	11.8	16.0	-0.4	19.7
$(\partial C/\partial P)_T$	0	12.9	8.9	2.1	12.3	10.0	-2.0	12.0
	0.015	-21.6	2.8	1.0				
	0.03	-7.9	4.0	0.6	-9.7	4.8	-1.7	-3.9

[a] $C=C_{\mu\nu}$ or B.

and to those derived from them by taking derivatives with respect to the pressure. The best fit was taken to be that which minimized the sum of the squares of the relative deviation between measured and calculated quantities in each case. Our results for $x=0.015$ and 0.03 are summarized in Table I, which also contains values for pure V_2O_3.[13] Also listed in Table I are 1-bar values and pressure derivatives of B, the bulk modulus, deduced from those of elastic constants using standard formulas.[31] As can be seen from Table I, the pressure derivatives of the elastic constants of Cr-substituted V_2O_3 are generally smaller than those of pure V_2O_3. Furthermore, the pressure derivatives of C_{11}, C_{12}, and B for the $x=0.03$ sample are all negative, as is the pressure derivative of C_{11} for the $x=0.015$ sample. The implications of these results will be discussed in the next section.

IV. DISCUSSION

A. Elastic stability under pressure

The criterion for the mechanical stability of a crystal, according to Born,[32] is that the elastic energy density be positive definite. This is equivalent to a condition that all the principal minors (or, alternatively, the eigenvalues) of the elastic-constant matrix should be positive. A negative pressure dependence of one of the elastic-constant eigenvalues would then imply that pressure causes the crystal to become less stable with respect to a certain elastic deformation. In view of the unusually negative pressure derivatives of some of the elastic constants for $(V_{1-x}Cr_x)_2O_3$ crystals (see Table I), it is appropriate to examine the behavior of the elastic-constant eigenvalues under pressure.

At room temperature $(V_{1-x}Cr_x)_2O_3$ has the corundum structure, which belongs to a trigonal crystal system with $\bar{3}m$ point-group symmetry.[3,7] The elastic-constant matrix contains six independent elements and has six distinct eigenvalues λ_i which can be expressed in terms of elastic constants as given in Ref. 14. The eigenvectors associated with eigenvalues λ_1, λ_2, λ_5, and λ_6 represent symmetry-breaking, shear deformations, while those associated with λ_3 and λ_4 represent combinations of longitudinal deformations which leave the $\bar{3}m$ symmetry invariant.[32]

Pressure derivatives of the eigenvalues were computed from the experimental pressure derivatives and 1-bar values of the elastic constants listed in Table I for V_2O_3 and $(V_{1-x}Cr_x)_2O_3$ with $x=0.03$. The relative change of each eigenvalue λ_i for these crystals is plotted in Fig. 3 as a function of applied hydrostatic pressure. It can be seen that in V_2O_3 all eigenvalues increase with pressure except λ_6 ($=C_{ST}$), which has a small negative pressure dependence. Although the behavior of λ_6 might seem to imply the occurrence of a transition to a triclinic structure at very high pressure, symmetry considerations[33] indicate that elastic deformation of the $\bar{3}m$ structure cannot by itself cause such a transition.

In $(V_{0.97}Cr_{0.03})_2O_3$, as can be seen from Fig. 3, λ_3 changes very little with pressure and λ_4 has a strong negative pressure dependence in contrast to the relatively large positive pressure dependences of both λ_3 and λ_4 in V_2O_3. The deformation characterized by the eigenvectors associated with λ_3 and λ_4 can be described by a symmetrized strain of the form[34]

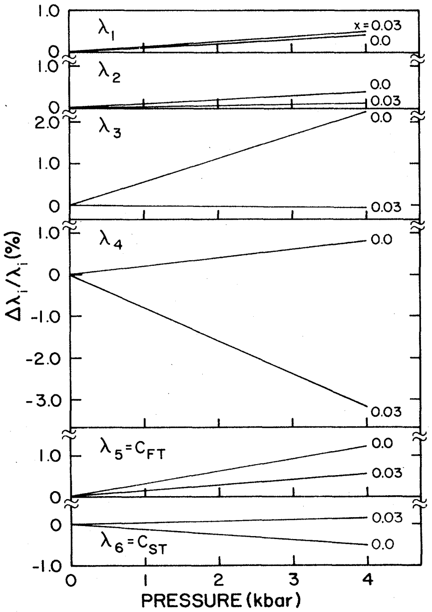

FIG. 3. Relative change of each eigenvalue λ_i as a function of hydrostatic pressure for $(V_{1-x}Cr_x)_2O_3$ with $x=0.0$ and 0.03.

$$\langle e \mid U_i \rangle = \alpha_i (e_1 + e_2) + \beta_i e_3 \ , \tag{2}$$

with

$$\frac{\beta_i}{\alpha_i} = \frac{2C_{13}}{\lambda_i - C_{33}} \ , \tag{3}$$

where $i = 3,4$ and U_i is an eigenvector associated with λ_i in a space spanned by strain components e_j ($j = 1-6$ in Voigt's notation). Since $\lambda_3 > C_{33}$ and $\lambda_4 < C_{33}$, $i = 3$ is essentially a dilatational deformation, while $i = 4$ corresponds to a stretching strain of tetragonal symmetry, consisting of extension (compression) along the threefold c axis and a uniform lateral compression (extension) in the basal plane perpendicular to the c axis, which changes the c/a ratio.

The pressure-induced decrease of the stability of $(V_{0.97}Cr_{0.03})_2O_3$ with respect to such a stretching deformation, indicated by the negative value of $\partial\lambda_4/\partial P$, is consistent with the fact that the pressure-induced IM transition proceeds without change in the crystal symmetry. In fact, x-ray-diffraction measurements[3] as a function of pressure on a powdered sample of $(V_{1-x}Cr_x)_2O_3$ with $x = 0.04$ revealed a discontinuous drop and rise in the a and c lattice parameters, respectively, at about the pressure where a resistivity discontinuity of more than 2 orders of magnitude was observed.[2,3]

The softening of λ_4 with increasing pressure in $(V_{0.97}Cr_{0.03})_2O_3$ can be seen to be caused primarily by $\partial C_{11}/\partial P$ and $\partial C_{12}/\partial P$ being negative in this material (in contrast to V_2O_3) since, using the fact that $(C_{11} + C_{12} - C_{33})^2 \ll 8C_{13}^2$, the expression for λ_4 in Ref. 14 can be approximated to give

$$\frac{\partial\lambda_4}{\partial P} \sim \frac{1}{2}\left[\frac{\partial C_{11}}{\partial P} + \frac{\partial C_{12}}{\partial P} + \frac{\partial C_{33}}{\partial P} - 2\sqrt{2}\frac{\partial C_{13}}{\partial P}\right] . \tag{4}$$

In the case of $(V_{0.985}Cr_{0.015})_2O_3$, as can be seen from Table I, sufficient data are lacking to determine the value of $\partial\lambda_4/\partial P$. Nevertheless, from the above considerations it seems reasonable to expect that the more negative value of $\partial C_{11}/\partial P$ in this sample than in the $x = 0.03$ sample may result in a more negative $\partial\lambda_4/\partial P$ for $x = 0.015$ than for $x = 0.03$ if $\partial C_{12}/\partial P \sim \partial C_{11}/\partial P$, as is true in V_2O_3 and $(V_{0.97}Cr_{0.03})_2O_3$. This suggests that $\partial\lambda_4/\partial P$ generally becomes more negative as the phase boundary is approached from the insulating side by decreasing x.

The slope of the IM phase boundary can be estimated from where the ultrasonic echoes disappeared, i.e., at a pressure of about 1 kbar at room temperature in the present work (see Sec. I) and at a temperature of about 250 K at atmospheric pressure in Ref. 16, to be $dT/dP \sim 50$ K/kbar. This is in fair agreement with the value of 40 K/kbar determined from electrical-resistivity measurements.[2]

It can also be seen from Table I that B has a negative-pressure dependence for the $x = 0.03$ sample—a new feature which has never been reported, to the authors' knowledge, for any crystalline solid. The only known example seems to be the bulk modulus of fused SiO_2,[35] which decreases strongly with pressure up to 20 kbar, where a collapse of the open oxygen network to a more dense modification occurs. Although B is not one of the eigenvalues of the elastic-constant matrix for a crystal with $\bar{3}m$ symmetry, the unusual softening of B with increasing pressure observed in $(V_{0.97}Cr_{0.03})_2O_3$ may be a precursor to the volume collapse of $\sim 1\%$ which accompanies the discontinuous change in the c/a ratio at the IM transition.

B. Elastic Grüneisen parameter

Anharmonic properties of solids are customarily described in terms of the Grüneisen parameter γ defined by

$$\gamma = \alpha_V B^S / C_P \ , \tag{5}$$

where α_V is the volumetric thermal-expansion coefficient, B^S the adiabatic bulk modulus, and C_P the heat capacity per unit volume at constant pressure. In the quasiharmonic approximation, in which atomic vibrations of a crystal are treated as a set of harmonic oscillators whose frequencies are volume dependent, Eq. (5) can also be expressed as a weighted average of the mode gammas $\gamma_i = -(\partial \ln\omega_i / \partial \ln V)$ as[36]

$$\gamma = \sum_{i=1} C_i \gamma_i \Big/ \sum_{i=1} C_i \ , \tag{6}$$

where C_i is the heat capacity of the ith normal mode with frequency ω_i and the summation is over the $3N$ normal modes of the crystal. The average in Eq. (6) can be reduced, in the anisotropic elastic continuum approximation, to a directional average of the acoustic modes (in the long-wavelength limit) whose mode γ's can be deduced from the elastic constants and their pressure derivatives.[36]

The thermal γ, determined from Eq. (5), has been found to agree with the elastic γ, computed from Eq. (6) in the continuum model, not only at temperatures much less than the Debye temperature Θ_D, but also when $T \gtrsim \Theta_D$ for a number of cubic[37,38] and hexagonal[9,39] crystals. It is, however, obvious that the elastic continuum approximation would be valid in the high-temperature limit only when the optical modes and the acoustic modes in the dispersive region have the same mode γ's as the low-frequency acoustic modes. Furthermore, in the case of $(V_{1-x}Cr_x)_2O_3$ crystals, which have relatively high Debye temperatures (calorimetric $\Theta_D = 580$ K for pure and Cr-substituted V_2O_3),[40] it is expected that not all the modes are completely excited at room temperature, so that they do not make equal contributions to the sum in Eq. (6). However, since the experimental heat capacity of $(V_{1-x}Cr_x)_2O_3$ can be reproduced by empirically fitting to a combination of Debye (D) and Einstein (E) functions as[40]

$$C_P \sim C_V = \tfrac{3}{5} Nk[D(\Theta_D/T) + 4E(\Theta_E/T)] \ , \tag{7}$$

where k is Boltzmann's constant and $\Theta_E = 465$ K for $T > 230$ K, we shall assume in view of Eq. (6) that

$$\gamma = \frac{3Nk}{5C_V}[\gamma_{ac} D(\Theta_D/T) + 4\gamma_{op} E(\Theta_E/T)] \ , \tag{8}$$

where γ_{ac} and γ_{op} are average acoustic- and optical-mode γ's, respectively. In the continuum approximation, γ_{ac} in

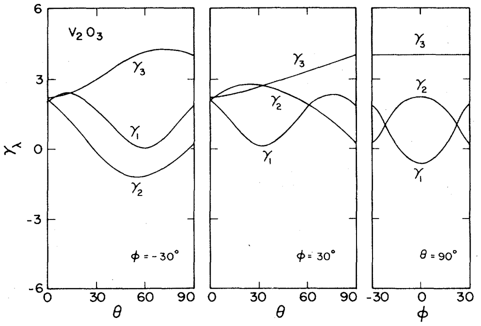

FIG. 4. Acoustic-mode γ_λ ($\lambda=1,2$ for transverse modes, $\lambda=3$ for longitudinal mode) deduced from elastic data along the three boundaries of the triangular zone formed by the (0,0,1), ($\sqrt{3}/2$, $-\frac{1}{2}$, 0), and ($\sqrt{3}/2$, $\frac{1}{2}$, 0) directions for V_2O_3.

Eq. (8) can be written in integral form as

$$\gamma_{\mathrm{ac}} \sim \gamma_{\mathrm{elas}} = \frac{1}{12\pi} \sum_{\lambda=1}^{3} \int \gamma_\lambda(\theta,\phi) d\Omega \ , \tag{9}$$

where $\gamma_\lambda(\theta,\phi)$ is the mode γ for an acoustic mode with polarization index λ and wave vector $\mathbf{q}$ in the direction of (θ,ϕ) and $d\Omega = \sin\theta\, d\theta\, d\phi$. It is therefore quite interesting to see how the thermal and elastic γ's differ from each other for the $(V_{1-x}Cr_x)_2O_3$ crystals, since any appreciable difference between the two can be largely attributed to the contribution from optical modes according to Eq. (8).

The mode γ's for the acoustic modes in crystals of trigonal symmetry can be deduced from the elastic constants and their pressure derivatives by means of the relation[39]

$$\gamma_\lambda(\hat{q}) = B^T \left[(l^2+m^2)\beta_\perp^T + n^2\beta_\parallel^T - \frac{1}{2} + \frac{1}{2} \left[\frac{\partial \ln W_\lambda}{\partial P} \right]_T \right] , \tag{10}$$

where $B^T = (2\beta_\perp^T + \beta_\parallel^T)^{-1}$ is the isothermal bulk modulus, (l,m,n) are the direction cosines of $\hat{q}$, and W_λ denotes the elastic modulus associated with the mode $(\lambda,\hat{q})$. A computer program was written for the Purdue CDC 6500 computer to calculate $\gamma_\lambda(\hat{q})$ as well as γ_{elas} in crystals of trigonal symmetry. With the elastic constants and their pressure derivatives as input data, the program computes W_λ and $\partial W_\lambda/\partial P$ in any direction of $\hat{q}$ by calculating the eigenvalues of the appropriate Christoffel tensors.[41] It is noted that, in view of the symmetry of the trigonal structure, it suffices to carry out the necessary numerical integration of $\gamma_\lambda(\theta,\phi)$ in Eq. (9) over only the directions confined to $\frac{1}{12}$ of a sphere bounded by three directions, (0,0,1), ($\sqrt{3}/2$, $-\frac{1}{2}$, 0), and ($\sqrt{3}/2$, $\frac{1}{2}$, 0), i.e., $0° \le \theta \le 90°$, $-30° \le \phi \le 30°$.[42]

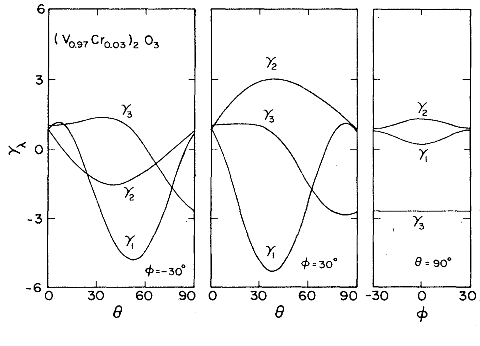

FIG. 5. Acoustic-mode γ's for $(V_{0.97}Cr_{0.03})_2O_3$ shown in the same way as in Fig. 4.

TABLE II. Room-temperature values of thermal and elastic Grüneisen parameters and the average optical mode γ for V_2O_3 and $(V_{0.97}Cr_{0.03})_2O_3$.

	γ_{th}[a]	γ_{elas}[b]	γ_{op}[c]
V_2O_3	1.61	1.64	1.60
$(V_{0.97}Cr_{0.03})_2O_3$	1.32	-0.78	1.85

[a] Deduced from thermal-expansion coefficients: References 3 (V_2O_3) and 28 [$(V_{0.97}Cr_{0.03})_2O_3$].
[b] Deduced from elastic data of Table I.
[c] Estimated from Eq. (8).

The above program was applied to V_2O_3 and $(V_{0.97}Cr_{0.03})_2O_3$. The resulting γ_λ for these crystals are shown in Figs. 4 and 5 along the three boundaries of numerical integration mentioned above, where $\lambda=1$ and 2 correspond to transverse modes and $\lambda=3$ is the longitudinal mode. In Table II the values of the Grüneisen γ's computed from thermal-expansion data are compared with the γ's computed from elastic data. Also given in Table II are the values of average optical-mode γ's estimated from Eq. (8). It is apparent that for V_2O_3 the corresponding thermal and elastic γ's are in excellent agreement, suggesting, in turn, the near equality of the average acoustic- and optical-mode γ's. In the case of $(V_{0.97}Cr_{0.03})_2O_3$, however, there is a large discrepancy between them. In fact, γ_{elas} is even negative, implying that γ_{op} is larger than γ_{th}. It can be seen from Fig. 5 that the negative γ_{elas} in $(V_{0.97}Cr_{0.03})_2O_3$ is caused by negative contributions from the $\lambda=1$ transverse mode and the $\lambda=3$ longitudinal mode. These are due to the $\lambda=1$ mode having a deep minimum for θ between 40° and 50°, apparently because of the negative pressure dependence of C_{QT} (see Fig. 2), and to the $\lambda=3$ mode becoming increasingly negative as the polar angle θ approaches 90° because of the negative pressure dependence of the C_{11} elastic constant. It is interesting to note that the softening of the C_{QT} modulus with pressure has been previously observed[20] in Ti_2O_3 and was attributed to an inherent instability of the cation sublattice in the corundum structure. It is not clear, however, why the C_{QT} mode softens with pressure in $(V_{0.97}Cr_{0.03})_2O_3$ but not in pure V_2O_3,[13] nor in $(Ti_{1-x}V_x)_2O_3$.[43]

V. CONCLUSION

Pressure derivatives of elastic constants are determined for $(V_{1-x}Cr_x)_2O_3$ with $x=0.015$ and 0.03. The strong negative pressure dependence of the λ_4 elastic eigenvalue derived therefrom implies that pressure causes a decrease in the stability of the corundum-structured lattice that is consistent with the abrupt increase in c/a ratio which occurs at the pressure-induced, insulator-to-metal transition. The disagreement between the thermal and elastic γ's of $(V_{0.97}Cr_{0.03})_2O_3$ is due to strong negative contributions from some of the long-wavelength acoustic modes.

ACKNOWLEDGMENT

This work was supported by the National Science Foundation via Materials Research Laboratory Program Grant No. DMR-80-20249.

---

[1] For a review of various properties of $(V_{1-x}Cr_x)_2O_3$, see, for example, J. M. Honig and L. L. Van Zandt, in *Annual Review of Materials Science,* edited by R. Huggins, R. H. Bube, and R. W. Roberts (Annual Reviews, Palo Alto, California, 1975), Vol. 5, p. 255.

[2] D. B. McWhan, T. M. Rice, and J. P. Remeika, Phys. Rev. Lett. **23**, 1384 (1969).

[3] D. B. McWhan and J. P. Remeika, Phys. Rev. B **2**, 3734 (1970).

[4] A. Jayaraman, D. B. McWhan, J. P. Remeika, and P. D. Dernier, Phys. Rev. B **2**, 3751 (1970).

[5] H. Kuwamoto, J. M. Honig, and J. Appel, Phys. Rev. B **22**, 2626 (1980).

[6] D. B. McWhan, A. Menth, J. P. Remeika, W. R. Brinkman, and T. M. Rice, Phys. Rev. B **7**, 1920 (1973).

[7] W. R. Robinson, Acta Crystallogr. Sect. B **31**, 1153 (1975).

[8] H. H. Demarest, Jr., R. Ota, and O. L. Anderson, in *High Pressure Research—Applications in Geophysics,* edited by M. H. Manghnani (Academic, New York, 1977), p. 281.

[9] E. Chang and G. R. Barsch, J. Phys. Chem. Solids **34**, 1543 (1973).

[10] I. L. Drichko and S. I. Kogan, Fiz. Tverd. Tela (Leningrad) **16**, 1015 (1974) [Sov. Phys.—Solid State **16**, 656 (1974)].

[11] G. O. Andrianov and I. L. Drichko, Fiz. Tverd. Tela (Leningrad) **18**, 1392 (1976) [Sov. Phys.—Solid State **18**, 803 (1976)].

[12] G. O. Andrianov, I. L. Drichko, and B. D. Laikhtman, Zh. Eksp. Teor. Fiz. **75**, 2246 (1978) [Sov. Phys.—JETP **48**, 1132 (1978)].

[13] D. N. Nichols and R. J. Sladek, Phys. Rev. B **24**, 3155 (1981).

[14] D. N. Nichols, R. J. Sladek, and H. R. Harrison, Phys. Rev. B **24**, 3025 (1981).

[15] S. A. Shivashanka, R. Aragon, H. R. Harrison, C. J. Sandberg, and J. M. Honig, J. Electrochem. Soc. **128**, 2472 (1981).

[16] H. Yang, R. J. Sladek, and H. R. Harrison, Solid State Commun. **47**, 955 (1983).

[17] Analyses performed by Galbraith Laboratories, Inc., P.O.Box 4187, Knoxville, TN 37921.

[18] S. Chen, J. E. Hahn, C. E. Rice, and W. R. Robinson, J. Solid State Chem. **44**, 192 (1982).

[19] E. P. Papadakis, J. Acoust. Soc. Am. **42**, 1045 (1967); H. J. McSkimin and P. Andreach, *ibid.* **34**, 609 (1962).

[20] D. S. Rimai, R. J. Sladek, and D. N. Nichols, Phys. Rev. B **18**, 6807 (1978).

[21] R. Truell, C. Elbaum, and B. B. Chick, *Ultrasonic Methods in Solid State Physics* (Academic, New York, 1969), App. A.

[22] J. B. Wachtman, Jr., W. E. Tefft, D. G. Lam, Jr., and R. P. Stinchfield, J. Res. Natl. Bur. Stand. Sect. A **64**, 213 (1960).

[23] M. H. Manghnani, J. Geophys. Res. **74**, 4317 (1969).

[24] D. S. Rimai, Phys. Rev. B **16**, 2200 (1977).

[25] D. S. Rimai and R. J. Sladek, Phys. Rev. B **18**, 2807 (1978).

[26] H. B. Huntington, in *Solid State Physics,* edited by F. Seitz and D. Turnbull (Academic, New York, 1958), Vol. 7, p. 213.

[27] This equation can be derived from the expression for linear compressibilities (Ref. 30) and the general relation between isothermal and adiabatic compliances (Ref. 26).

[28] G. V. Chandrashekar and A. P. B. Sinha, Mater. Res. Bull. **9**, 787 (1974).

[29] H. V. Keer, H. L. C. Barros, D. L. Dickerson, A. T. Barfknecht, and J. M. Honig, Mater. Res. Bull. **12**, 137 (1977).

[30] J. F. Nye, *Physical Properties of Crystals* (Oxford University Press, London, 1972), p. 131.

[31] O. L. Anderson, J. Phys. Chem. Solids **27**, 547 (1966).

[32] M. Born and K. Huang, *Dynamical Theories of Crystal Lattices* (Oxford University Press, London, 1954), p. 129.

[33] N. Boccara, Ann. Phys. (Leipzig) **47**, 40 (1968).

[34] The sign of the last term in Eq. (2) is the opposite of that given in Ref. 14, which is in error.

[35] E. H. Bogardus, J. Appl. Phys. **36**, 2504 (1965).

[36] See, for example, J. C. Slater, *Introduction to Chemical Physics* (McGraw-Hill, New York, 1939), p. 199.

[37] F. W. Sheard, Philos. Mag. **3**, 1381 (1958); J. G. Collins, *ibid.* **8**, 323 (1963).

[38] K. Brugger and T. C. Fritz, Phys. Rev. **157**, 524 (1967).

[39] D. Gerlich, J. Phys. Chem. Solids **30**, 1638 (1969). Although, in Ref. 39, Eq. (10) of this text was derived for the tetragonal and hexagonal crystals, it can be shown that Eq. (10) is valid for any uniaxial crystal, including the trigonal $\bar{3}m$ for which $C_{24}=-C_{14}$.

[40] H. V. Keer, D. L. Dickerson, H. Kuwamoto, H. L. C. Barros, and J. M. Honig, J. Solid State Chem. **19**, 95 (1976).

[41] W. P. Mason, *Physical Acoustics and the Properties of Solids* (Van Nostrand, Princeton, N.J., 1958), p. 355.

[42] G. A. Alers, in *Physical Acoustics,* edited by W. P. Mason (Academic, New York, 1965), Vol. III B, p. 1; Ref. 22.

[43] D. N. Nichols, D. S. Rimai, and R. J. Sladek, Phys. Rev. B **25**, 3786 (1982).